Surface Enhanced Raman Spectroscopy of Phenolic Antioxidants: A Systematic Evaluation of Ferulic Acid, p-Coumaric Acid, Caffeic Acid and Sinapic Acid

Iris Aguilar-Hernández[1], Nils Kristian Afseth[2], Tzarara López-Luke[3], Flavio F. Contreras-Torres[1], Jens Petter Wold[2], Nancy Ornelas-Soto[1*]

[1] Tecnológico de Monterrey, Laboratorio de Nanotecnología Ambiental, 64849, Monterrey, Nuevo León, México.

[2] Nofima AS – Norwegian Institute of Food, Fisheries and Aquaculture Research, Muninbakken 9-13, Breivika, NO-9291 Tromsø, Norway.

[3] Centro de Investigaciones en Óptica, León, Gto., C.P. 37150, México.

Abstract

Surface-Enhanced Raman Spectroscopy (SERS) is a powerful surface-sensitive technique to study the vibrational properties of analytes at very low levels of concentration. In particular, detection of bioactive molecules, specifically antioxidants, is an area of interest to gain insights into the reproducible and quantitative SERS-determination. In this study, SERS measurements were systematically evaluated for ferulic acid, p-coumaric acid, caffeic acid and sinapic acid. The study objective in this research was to: 1) prepare and characterize SERS-active silver colloids; 2) cluster the as-obtained colloids through Principal Component Analysis on the basis of concentration and nanoparticle size; and 3) develop a highly sensitive SERS-based method for phenolic antioxidant detection. The reliability of the proposed method was demonstrated through detection of the phenolic antioxidants evaluated at low levels of concentration. In particular, sinapic acid was evaluated for the first time, with a limit of detection of 2.5×10^{-9} M.

Keywords: SERS, phenolic antioxidants, sinapic acid, ferulic acid, p-coumaric acid, caffeic acid

Corresponding Author: ornel@itesm.mx

1. Introduction

Ferulic acid, p-coumaric acid, caffeic acid and sinapic acid (see Scheme 1) are examples of important natural phenolic antioxidants [1]. Due to the potential beneficial effects of these compounds regarding human health, considerable evidence about other properties such as UV-protection, anti-carcinogenic and anti-inflammatory properties, as well as cardiovascular protection have been reported [2–5]. Phenolic acids are rarely found in their free forms [6,7]. Nonetheless, studies indicate that free phenolic compounds show an increase of their antioxidant capacity. Other studies about bioavailability indicate that free ferulic acid can be absorbed along the entire gastrointestinal tract, furthermore, free p-coumaric acid is also rapidly absorbed, but in an intact form [7]. Moreover, these compounds by themself, have many industrial applications, for example, they can be used as natural preservatives for foods, and applied in the production of paints, paper, and cosmetics [8]. Therefore, there is an increasing development of methods for liberation of natural antioxidants from plant materials for industrial applications [9,10]. Characterization and quantification of phenolic compounds can be determined by various analytical instrumental methods of which liquid chromatography is the technique of choice, allowing to reach limits of detection in the order of 10^{-8} to 10^{-12} M [11–16]. However, in some cases, factors such as costs, real-time implementation of analysis, assortment of standards, use of solvents and pretreatment of samples can restrict the use of chromatography methods, thus limiting a high-throughput analytical quality control [17].

Raman spectroscopy is a well-known non-destructive vibrational technique for structural analysis and quantification of molecules. The fast analytical response and the safe contextual analysis to get measurements leading to a non-intrusive property [18–20] are only limited by the low scattering

efficiency [21] which can restrict its applicability for analytes at low levels of concentration. To enhance the Raman scattering efficiency [22,23], the use of 'free-electron-like' particles of noble metals (e.g., Ag, Au) in the 10–100 nm size range is a procedure to create hot electrons that ultimately interact with the analyte to produce resonant vibronic coupling of the adsorbate's vibration to the plasmon's transition dipole [24–28]. Such mechanism requires the formation of a metal–adsorbate chemical bond, sometimes referred as a first-layer effect [29]. Over the years, surface enhanced Raman scattering (SERS) has proven to be a powerful platform for the quantitative trace analysis of a large number of biomolecules including amino acids [30–32], proteins [33–35], DNA [36,37], and *in vivo* detection of analytes in cellular environments [38–41]. Owing to the benefits of using the SERS technique for quantitative detection of important bioactive molecules [42–45] several factors have to be taken into consideration [46]. In particular nanoparticle size, shape and aggregation, as well as the type of substrate (e.g., colloids and solid state) employed, and the pH of the solution studied are subjected to a more refined quality assessment to gain a criteria of sensitivity [47]. A survey of the literature reveals that a few SERS-based studies were focused on the collection of quantitative results in which the limits of detection have been well established [34,48–51].

The main objective of this study was to develop a SERS method for the identification of four free phenolic antioxidants, namely, ferulic acid, p-coumaric acid, caffeic acid and sinapic acid. Principal Component Analysis (PCA) was applied and performed to classify the as-prepared silver colloids based on the concentration of reagent employed and the nanoparticle size obtained (including their aggregation). Semi-quantitative analysis with glycine as the probe molecule was carried out to gain an insight into the sensitivity in the SERS-determination for the phenolic compounds. The method proposed is more sensitive for detection of p-coumaric acid and caffeic acid than previous reports [42–45,52] in which the limits of detection are within the range of 10^{-3} to 10^{-4} M. In this study, for the first time, the SERS-detection of sinapic acid is reported; the lowest limit of detection reached was in the

order of 10^{-9} M.

2. Experimental

2.1 Chemicals and reagents

Silver nitrate ($AgNO_3$, 99%), sodium borohydride ($NaBH_4$, 99%), glycine (Gly, 99%), ferulic acid (4-hydroxy-3-methoxy cinnamic acid, >98%), p-coumaric acid (3-(4-hydroxyphenyl)-2-propenoic acid, >98%), caffeic acid (3-(3,4-dihydroxyphenyl)-2-propenoic acid, >98%), sinapic acid (4-hydroxy-3,5-dimethoxy-cinnamic acid, >98%), nitric acid (HNO_3, 70%) and ethanol analytical pure reagent were purchased from Sigma–Aldrich. All the reagents are reactive grade and were used without additional purification. When it was required, aqueous solutions were prepared using ultrapure water (18.2 MΩ cm^{-1}) purified with a Milli-Q® System (Millipore Corp., USA).

2.2 Preparation of SERS-active silver colloids

Silver colloids were prepared by a modified Creighton method [53]. A stock solution was made by adding 10 mL of $AgNO_3$ (3.5 mM) dropwise to 30 mL of freshly prepared $NaBH_4$ solution (7 mM) cooled in an ice bath. The reaction was carried out in an open system under continuous stirring for 3 min [54]. Aging of the stock solution after synthesis was varied from 15 to 80 min, a factor that can influence in the size and aggregation of colloidal particles produced. Afterwards, aliquots of stock solution were transferred to clean beakers and diluted with deionized water to attain the final concentrations. A total number of 41 different silver colloidal suspensions were prepared by varying both the aging and final concentration (Table 1), which all were kept in darkness. No additional stabilizing agents besides excess $NaBH_4$ were used in order to prevent undesirable salt-mediated reactions [55].

2.3 Silver colloid characterization

The formation of silver nanoparticles (AgNPs) was confirmed by UV-Vis spectroscopy and transmission electron microscopy (TEM). All the UV-Vis absorption spectra of the silver colloidal

solutions were obtained over the region from 325 to 550 nm using a photodiode array Agilent 8453 UV-Visible spectrophotometer (Agilent Technologies, Waldbronn, Germany). The morphology of AgNPs was investigated with a Morgagni 268 electron microscope (FEI, Co) operated at 80 kV.

TEM samples were prepared by casting 5 mL of selected colloidal samples onto carbon coated copper grids (Ted Pella, Redding, CA). Excess solution was then removed with paper filter and dried at room temperature for approximately 60 min. The average diameters of the nanoparticles were determined using ImageJ 1.43u software (Wayne Rasband National Institutes of Health, USA).

2.4 Principal Component Analysis

UV-Vis absorption spectra measurements taken from silver colloidal suspensions were analyzed by Principal Component Analysis (PCA) to cluster the colloids synthesized with different concentration of precursor and aging period of the stock solution. PCA is a useful statistical tool to estimate the effect of the preparation of colloids since PCA can reduce the dimensionality of a data set by finding an alternative set of coordinates called principal components [56]. This analysis linearly transforms a data matrix, which contains information related to the UV-Vis absorption spectra, to new variables of few dimensions (e.g., concentration of reagents, nanoparticle size and aggregation). Thus the PCs are ranked according to their variance; PC1 corresponds to the new variable with the maximum variance (i.e., concentration of silver), and PC2 is the second variable (i.e., size of AgNPs) that contains all of the information not included in PC1. The score values of the principal components were used to associate the as-obtained silver colloids in clusters according to trends in the data obtained. Data analysis was carried out using The Unscrambler® X version 10.1 software package.

2.5 Surface-enhanced Raman spectra measurements

SERS measurements were acquired using a LabRam HR 800 Raman spectrometer (Horiba Scientific, France) equipped with a He-Ne laser (15 mW) operating at 633 nm. A 40 mm objective lens was used for sample focusing; the collection of Raman spectra were accumulated over 4 s. Scattered light was

collected by a CCD camera thermoelectrically cooled at –70 ºC. Raman scattering was dispersed with a 200 lines/mm grating, which resulted in spectra in the range from 400 to 2600 cm^{-1}. SERS spectra were recorded in 1-mL quartz cells filled with silver colloidal mixed with the required amount of analyte.

2.5 Analysis of antioxidants

The effect of pH on the SERS enhancement was studied by mixing each analyte (FA, 4CA, CA and SA) with the silver colloid to obtain a final concentration of $7.5x10^{-6}$ M. The concentration was fixed, and pH was varied in a range from 2 to 12 using HNO_3. The pH of the solution was measured with a pH meter.

For studying the variation of SERS spectra with concentration, a stock solution of $1x10^{-2}$ M of each analyte and silver colloid were mixed in a final volume of 1 mL, to obtain working concentrations between 2.5×10^{-9} M and 7.5×10^{-6} M. pH of the solution was 6.5, 6.3, 5.5 and 6.3 for FA, 4CA, CA and SA, respectively.

The area under the curve of each SERS spectra was calculated in the range of 1100 to 1700 cm^{-1} using the Origin 9.1 software package.

3. Results and discussion

3.1 Characterization of silver colloids

Aging time of the stock solution can allow the formation of individual nanoparticles of different sizes [30]. Subsequent dilution can induce precipitation [57] since the concentration of $NaBH_4$ is reduced. Such differences can be highlighted as the systematic changes observed in the shape of the UV-Vis absorption bands (e.g., broadening absorbance peak, shoulders and λmax shifts). The UV-Vis absorption spectra of the colloidal suspensions are shown in Figure 1A. It can be observed that the position of the main surface plasmon resonance peak is located at around 390 nm, providing evidence of AgNPs formation. Also, a pale yellow solution is a good indication that the chemical reaction took place and that the seeds available in the solution ranges from 5 to 20 nm in diameter, in agreement with

previous studies reported elsewhere [30,58]. In Figure 1A, the sharpness of some peaks suggests the uniqueness of the particle-size when the peak width half medium (PWHM) is approximately 25 nm. On the other hand, the existence of colloids with several particle sizes was observed through the formation of dark-brown color solutions, in which their corresponding absorption bands show the emergence of shoulders, which can be related with the presence of particles of different size [59,60]. A red shift in the λ_{max} indicated the formation of larger particles [61,62] whose bands of absorption are broader and located at 406 nm.

PCA analysis was carried out to cluster the colloidal suspensions according to variances in concentration, aggregation and size of nanoparticles. Table 1 shows the conditions of preparation of the used colloids. As observed in Figure 1C, the score plot of PC1 (88% of the total variance) *versus* the score plot of PC2 (9% of the total variance) separates the colloids in clusters that were grouped in the four quadrants. Samples of colloids observed in both the left and right side (e.g., colloids 3, 6, 8, 9, 11, 12, 14, 16, 28, etc.) were not clustered by the PCA since they correspond either the lowest or the highest concentrations tested respectively. However, several colloids were clustered at the center of the plot, which can be distinguished by variances along the PC1 and PC2 axes. In particular, the PC2 axis spans the variation in the nanoparticle size and aggregation, from large-aggregated (bottom) to small (top). The colloids prepared with a intermediate values of concentration are located at the center, namely, (A) the colloids obtained within an aging period of 60-80 min, which showed a largest nanoparticle sizes and aggregation ($-2 < PC2 < -1$); (B) the colloids obtained within a period between 15 and 30 min, which showed medium nanoparticle sizes ($-0.5 < PC2 < 0.5$); and finally (C) the colloids obtained within aging periods from 45-60 minutes, which exhibited the smallest nanoparticle sizes ($0.5 < PC2 < 1.5$). In the synthesis of the colloids, the reducer is also used as stabilizer ($NaBH_4$), therefore, the aging time affects not only the aggregation but also the nanoparticle size. These features confer together differentiation among UV spectra, which is reflected in the PCA study.

Representative TEM images of silver colloids are shown in Figure 1B. Although sample preparation for TEM measurements can impact the morphology of the nanoparticles, this technique has been used to reinforce the observations derived from the UV-spectra analysis regarding size and nanoparticle aggregation between selected colloids [30]. It was observed that AgNPs are predominantly spherical in shape. The profile measurements showed that the diameter of these particles is roughly 2-15 nm (small size), 3-20 nm (medium size) and 8-30 nm (large size). Moreover a lower degree of aggregation was observed for the colloids in which individual particles display an average size of about 8.5±3 nm (Fig.

1B, left), while the colloids with larger particles of 19.0 ± 2 nm showed a high level of aggregation (Fig. 1B, right). These observations suggested that the aging period of the stock solution could induce changes in the size and aggregation of the AgNPs.

3.2 Evaluation of SERS-active silver colloids with a probe molecule

Selected silver colloids from PCA clusters A, B and C, as well as non-clustered colloids were used to test the SERS activity using glycine (Gly) as a probe molecule with well known Raman and SERS peaks [63–65] in order to identify the optimal conditions of colloidal synthesis which allows the formation of hotspots caused by particle aggregation [66] and their further use for study of antioxidants.

The enhancement in the intensity of glycine (2.5×10^{-3} M) by using different AgNPs colloids against normal Raman scattering (1M) is shown in Fig. 2. The pH for all the synthesized colloids was adjusted to a value of 8.0 to promote deprotonation of COOH (pKa = 2.3, carboxylate) [30,31,63]. Therefore, the interaction of Gly with AgNPs was highly improved using a higher population of molecules with negative partial charges (i.e., Gly anion). As compared to the corresponding Raman spectrum, the SERS enhancement observed can be particularly remarked for the peak assigned to a symmetric stretching vibration for the carboxylate group ($–COO^–$) at ~1382 $cm^{–1}$. Such vibration corresponds to the adsorption of the amino acid onto the surface of AgNPs through the carboxylate [63]; there is no indication of the 1600-$cm^{–1}$ vibration related to the carboxyl group (–COOH) [64]. As Fig. 2 shows, the highest SERS intensities were obtained for colloids located at PC1>0, while lowest intensities were obtained for colloids located at PC1< 0. In particular, high intensities were observed for the colloids 2 and 7 located in cluster A. Moreover, it was observed that low nanoparticle concentration (e.g., colloids 6 and 8) produced no significant signals. According to PCA analysis, those colloids have a suitable nanoparticle size to allow detection of analytes at very low levels of concentration, nonetheless, a certain degree of nanoparticle aggregation [56], [57] is needed in order to obtain the enhancement.

PCA analysis (PC2 < 0) suggested that the colloids obtained by aging stock solution between 60 and 80 min and high concentration can produce the highest enhancement of SERS signals (e.g. colloid 12). Therefore one of the most critical parameter on the SERS enhancement is the nanoparticle aggregation, possibly due to the number of active sites upon which the analytes are adsorbed, as reported for molecules like nile blue [67] caffeine [54], tryptophan ([30] and proteins [48].

3.3 SERS-based method for systematic evaluation of antioxidants

SERS spectra of ferulic acid (FA), p-coumaric acid (4CA), caffeic acid (CA) and sinapic acid (SA) obtained with silver colloidal solutions are shown in Figure 3. Initially, the SERS-active silver colloids tested were the samples 7, 2, 12, allocated in those variances representing the values PC1> 0 and PC2 <0 since they have shown high performance for SERS effect (data not shown). Finally, colloid 12 was employed for all further experiments with antioxidants. In Figure 3, FA, 4CA, CA and SA analytes were used with a concentration of 7.5×10^{-6} M, which was the highest concentration analyzed by SERS technique in this work, and where the peaks are more defined for their respective assignment. For comparison, the normal Raman spectra were obtained from a film made by drop casting an aliquot of 1 M solution of antioxidants molecules onto aluminum substrates and followed by air-drying. The background (i.e., silver colloids) level is as low as constant that do not contribute to the signals detected. Band assignments obtained from Raman and SERS measurements are provided in Table 2.

The main characteristic bands located in the SERS spectra are the stretching-type modes of the $–COO^-$ moieties and C=C bonds that leads to deformation of phenyl rings. The symmetric $–COO^-$ stretching appeared at 1360, 1372, 1351 and 1345 cm^{-1} while the C=C [52,68] stretching were observed at 1521, 1584, 1492 and 1580 cm^{-1} for FA, 4CA, CA and SA analytes, respectively. The phenyl ring deformations appeared as intense bands at 1605, 1622, 1605 and 1624 cm^{-1} in the corresponding spectrum. The bands located at 1126, 1162, 1164 and 1156 cm^{-1} can be attributed to in-plane C–H bending vibrations, while the bands at 958, 977, 969 and 973 cm^{-1} may be assigned to out-of-plane C–

H bending vibrations for FA, 4CA, CA and SA, respectively. The difference observed in the wavenumbers and relative intensities is explained in terms of physical adsorption of the analytes to the AgNPs surface [69,70]. For instance, the presence of the band in the region 1370-1340 cm^{-1} pointed out a possible interaction via the carboxylate group. However, a close inspection reveals that the adsorption can also take place through other different conformations. This is the case for CA, in which the existence of two bands in the region 580-480 cm^{-1} suggested that the adsorption occurred through the *o*-diphenyl moiety, and thus the analyte can be adsorbed to AgNPs through a perpendicular orientation [46]. Moreover, the appearance of a high intensity band seen at 485 cm^{-1} was related to polymerization of CA [45]. In the case of FA, the SERS spectrum also showed the aforementioned bands but in contrast to CA, a broader and low intensity band was observed at about 550-500 cm^{-1}. In the cases of 4CA and SA, there was observed only a weak band at 561 and 502 cm^{-1}, respectively. The evident change observed at this region is a consequence of the chemical nature of the analytes, and thus can be directly dependent of the sum of the surface effects (e.g., electronic effects, steric hindrance and pH of the solution). Finally, the normal Raman spectra for each antioxidant (1 M) were obtained and compared to the corresponding SERS spectrum (1×10^{-6} M). The SERS enhancement factor ($EF = I_{SERS}/I_R \times C_R/C_{SERS}$) was calculated for the peak at about 1610 cm^{-1} and thus was estimated to be approximately 5.4×10^5. This definition is particularly suited to the case of SERS active liquids such as the case of colloidal solutions [71].

Figure 4 shows the pH dependence for SERS spectra of phenolic antioxidants obtained in the pH range of 2 to 12. The SERS spectra were obtained and the areas were calculated for the spectral region between 1100 and 1700 cm^{-1}. This range was used to calculate absolute SERS enhancement, since the pH variations could affect the molecular conformation of the analyte and hence its interaction with the colloid surface. The maximum areas were observed at pH values from 5.0 to 6.5. The SERS spectra changed at different pH values, which suggested that the adsorption orientation on nanoparticles is pH-

dependent [72]. Based on the pKa values [73] corresponding to the –COOH groups of the antioxidants analyzed (see Scheme 1), the latter indicated that the chemical analyte–AgNPs interaction occurred in anionic form (i.e., such as a carboxylate), as observed for Gly. At the more acidic pH values, the overall spectral quality is totally modified giving rise to smaller areas. Those changes in the spectrum can be attributed to decomposition of analytes. However, it is also well known that SERS spectra are elusive to detection because of the instability of colloids under extreme pH conditions [74]. Therefore, a less dramatically change in the SERS spectra was observed up to pH values within 7 and 7.5, which suggested the interaction of carboxylate group. It is noteworthy that other anionic species can be formed due to partial deprotonation of the –OH groups. Taking into account the second pKa value [73] of the antioxidants studied, it was observed that very weak bands in the SERS spectrum were obtained at pH > 9 values. For the case of CA, enhancement of SERS signals were observed at basic pH values within 8 and 10, probably due to a reorientation of analyte on the silver surface. Thus, the enhancement in the SERS spectra was corroborated by the appearance of a strong band attributed to the phenol ν(C–O) stretching vibration located at 1219, 1238, 1221 and 1284 cm^{-1} for FA, 4CA, CA and SA, respectively. The adsorption of the second anionic structure onto AgNPs may stabilize the phenolate form of antioxidants; however experimental limitations hinder the observation of a possible Ag–O interaction (~250-350 cm^{-1})[75,76]. As a whole, these results pointed out the importance of the pH value to attain reproducible SERS spectra when using silver colloidal solutions.

Figure 5 shows the SERS detection at different levels of concentration of analytes. The SERS spectra cover a concentration range between 7.5×10^{-6} M and 2.5×10^{-9} M. As described above, the largest SERS enhancements were obtained for dilute solutions of antioxidants that were particularly adjusted to those pH values. The SERS spectra of SA, FA, 4CA and CA were recorded at 6.3, 6.5, 6.3 and 5.5 pH value, respectively. The low-concentration (2.5×10^{-9} M) spectra showed two characteristic bands

observed at about 1360 and 1610 cm^{-1} and attributable to ν_s(COO–) and in-plane C=C stretching mode, respectively. On the other hand, the SERS spectra of SA were recorded at pH 6.1. The SERS spectrum of SA showed an intense band located at 1452 cm^{-1} attributable to $–OCH_3$ bending. However fluctuations of the SERS intensities at concentrations lower than 1×10^{-8} M were observed. Differences in the relative intensities recorded can be explained in terms of chemical adsorption of the analytes to AgNPs. Due to steric hindrance of the $–OCH_3$ groups, which are adjacent to –OH group, SA can be only adsorbed to AgNPs through a nonperpendicular orientation. The interaction between the ring and the silver surface is supported by the strong intensity of the C=C ring stretching mode observed at 1605 cm^{-1}, which is clearly visible at higher concentrations. However, the orientation of SA is quite difficult to determine due to the analyte keeps very low symmetry (Cs point group).

To verify the univariate linear dependence of the SERS-based method, calibration curves were obtained by plotting the SERS intensities of the SERS spectra against the antioxidant concentration in a range from 2.5×10^{-9} M to 7.5×10^{-6} M.

Figure 6A and 6B shows graphs of concentration versus areas, which were calculated for the spectral region between 1100 and 1700 cm^{-1}. For the purpose of semi-quantitative detection, high sensitivity was observed for CA, 4CA, FA and SA. However, there is no significant correlation at low concentrations, as shown in Fig. 6A. These results can be attributed to the chemical structure of the analytes, which should cover the surface of nanoparticles only at a submonolayer level [77]. Particularly, despite the lack of correlation at low concentrations of SA, this is the first study in which this phenolic antioxidant was detected by a SERS method, with a limit of detection in the order of $1x10^{-9}$ M. In the case of higher concentrations of analyte (Figure 6B), a dependence of the SERS spectra on the concentration was observed, with correlation coefficients of 0.993, 0.986, 0.945, 0.989 for CA, 4CA, FA and SA, respectively.

4.Conclusions

A PCA analysis was employed as a useful tool to cluster the colloids prepared in this work on the basis of their concentration aggregation and nanoparticle size, in order to gain insights into the sensitive and quantitative SERS determination. Tests with diverse colloids show that not any colloidal solution can generate sensitive SERS measurements; some of them offered poor levels of enhancement or produced no signal at all, even when working with a test molecule like the amino acid glycine. Selected conditions for colloidal synthesis such as high concentration and long aging times (Table 1) were used for the development of a highly sensitive SERS-based method for the detection of ferulic acid, p-coumaric acid, caffeic acid, and sinapic acid. The prepared SERS-active silver colloids showed an effective enhancement of Raman signals allowing the sensitive detection of the analytes at low concentrations ($2.5x10^{-9}$M). For 4CA and CA, these low detections were reached for the first time. In addition, the SERS analysis of SA using silver colloids is also detected for the first time. Moreover,It was observed that the enhancement of SERS signals was highly dependent on pH, and subsequently on the chemical structure of each analyte at a specific pH value and its interaction with the surface of the metallic nanoparticles

Acknowledgements

Financial support from National Council of Science and Technology of Mexico (CONACyT) through grant 183743, PEI 230785 and scholarship #400488 is greatly appreciated.

References

[1] T.P. Kondratyuk, J.M. Pezzuto, Arch. Physiol. Biochem. 42 (2004) 46–63.

[2] M. Srinivasan, A.R. Sudheer, V.P. Menon, J. Clin. Biochem. Nutr. 40 (2007) 92–100.

[3] C. Luceri, L. Giannini, M. Lodovici, E. Antonucci, R. Abbate, E. Masini, P. Dolara, Br. J. Nutr.

97 (2007) 458–63.

[4] M. Touaibia, J. Jean-François, J. Doiron, Mini Rev. Med. Chem. 11 (2011) 695–713.

[5] N. Nićiforović, H. Abramovič, Compr. Rev. Food Sci. Food Saf. 13 (2014) 34–51.

[6] A.H. Laghari, S. Memon, A. Nelofar, K.M. Khan, A. Yasmin, Food Chem. 126 (2011) 1850–1855.

[7] A. Ota, H. Abramovič, V. Abram, N. Poklar Ulrih, Food Chem. 125 (2011) 1256–1261.

[8] K. Hayat, X. Zhang, H. Chen, S. Xia, C. Jia, F. Zhong, Sep. Purif. Technol. 73 (2010) 371–376.

[9] V.A. Papillo, P. Vitaglione, G. Graziani, V. Gokmen, V. Fogliano, J. Agric. Food Chem. 62 (2014) 4119–4126.

[10] A. de Camargo, M.A.B. Regitano-d'Arce, C. Telles Biasoto, F. Shahidi, Food Chem. 212 (2016) 395–402.

[11] V. Nour, I. Trandafir, S. Cosmulescu, J. Chromatogr. Sci. 51 (2013) 883–890.

[12] A. Zhang, L. Wan, C. Wu, Y. Fang, G. Han, H. Li, Z. Zhang, H. Wang, Molecules 18 (2013) 14241–14257.

[13] J. Yang, P.D. Bowman, S.M. Kerwin, S. Stavchansky, Biomed. Chromatogr. 28 (2014) 241–246.

[14] B. Bayram, B. Ozcelik, G. Schultheiss, J. Frank, G. Rimbach, Food Chem. 138 (2013) 1663–1669.

[15] E. Porgali, E. Büyüktuncel, Food Res. Int. 45 (2012) 145–154.

[16] A.M. Tarola, F. Van de Velde, L. Salvagni, R. Preti, Food Anal. Methods 6 (2013) 227–237.

[17] P. Bourget, A. Amin, F. Vidal, C. Merlette, F. Lagarce, J. Pharm. Biomed. Anal. 91 (2014) 176–184.

[18] A. Jenkins, R. Larsen, T. Williams, Spectrochim. Acta. A. Mol. Biomol. Spectrosc. 61 (2005) 1585–94.

[19] S.-M. Choi, C.-Y. Ma, Food Chem. 102 (2007) 150–160.

[20] K. Virkler, I. Lednev, Forensic Sci. Int. 181 (2008) e1–e5.

[21] B. Pettinger, in:, J. Lipowski, P.N. Ross (Eds.), Adsorpt. Mol. Met. Electrodes, 1992, p. 285.

[22] D.L. Jeanmaire, R.P. Van Duyne, J. Electroanal. Chem. Interfacial Electrochem. 84 (1977) 1–20.

[23] M.G. Albrecht, J.A. Creighton, J. Am. Chem. Soc. 99 (1977) 5215–5217.

[24] M. Moskovits, Rev. Mod. Phys. 57 (1985) 783–826.

[25] L. Jensen, C.M. Aikens, G.C. Schatz, Chem. Soc. Rev. 37 (2008) 1061–1073.

[26] J.R. Lombardi, R.L. Birke, J. Phys. Chem. C 112 (2008) 5605–5617.

[27] J.R. Lombardi, R.L. Birke, Acc. Chem. Res. 42 (2009) 734–742.

[28] C.L. Haynes, C.R. Yonzon, X. Zhang, R.P. Van Duyne, J. Raman Spectrosc. 36 (2005) 471–484.

[29] M. Moskovits, Phys. Chem. Chem. Phys. 15 (2013) 5301–11.

[30] A. Kandakkathara, I. Utkin, R. Fedosejevs, Appl. Spectrosc. 65 (2011) 507–13.

[31] X. Dou, Y.M. Jung, H. Yamamoto, S. Doi, Y. Ozaki, Appl. Spectrosc. 53 (1999) 133–138.

[32] F. Wei, D. Zhang, N.J. Halas, J.D. Hartgerink, J. Phys. Chem. B 112 (2008) 9158–64.

[33] E. Podstawka, Y. Ozaki, L.M. Proniewicz, Appl. Spectrosc. 58 (2004) 1147–56.

[34] O. Dong, D.C.C. Lam, Mater. Chem. Phys. 126 (2011) 91–96.

[35] X.X. Han, H.Y. Jia, Y.F. Wang, Z.C. Lu, C.X. Wang, W.Q. Xu, B. Zhao, Y. Ozaki, Anal. Chem. 80 (2008) 2799–804.

[36] J.V. García-Ramos, S. Sánchez-Cortés, J. Mol. Struct. 405 (1997) 13–28.

[37] Y. He, S. Su, T. Xu, Y. Zhong, J.A. Zapien, J. Li, C. Fan, S.-T. Lee, Nano Today 6 (2011) 122–130.

[38] T. Smith-Palmer, C. Douglas, P. Fredericks, Vib. Spectrosc. 53 (2010) 103–106.

[39] N.E. Marotta, L.A. Bottomley, Appl. Spectrosc. 64 (2010) 601–606.

[40] G. V Pavan Kumar, B. a Ashok Reddy, M. Arif, T.K. Kundu, C. Narayana, J. Phys. Chem. B 110 (2006) 16787–92.

[41] E. Cepeda-Perez, I. Aguilar-Hernandez, T. Lopez-Luke, V. Piazza, R. Carriles, N. Ornelas-Soto, E. de la Rosa, Appl. Spectrosc. (2016).

[42] R.E. Clavijo, D.J. Ross, R.F. Aroca, J. Raman Spectrosc. 40 (2009) 1984–1988.

[43] S. Sánchez-Cortés, J. V. García-Ramos, Appl. Spectrosc. 54 (2000) 230–238.

[44] S. Sánchez-Cortés, J. V. García-Ramos, Spectrochim. Acta - Part A Mol. Biomol. Spectrosc. 55 (1999) 2935–2941.

[45] S. Sánchez-Cortés, J. García-Ramos, J. Colloid Interface Sci. 231 (2000) 98–106.

[46] M. Sackmann, a. Materny, J. Raman Spectrosc. 37 (2006) 305–310.

[47] D. Zhang, R. Haputhanthri, S.M. Ansar, K. Vangala, H.I. De Silva, A. Sygula, S. Saebo, C.U. Pittman, Anal. Bioanal. Chem. 398 (2010) 3193–3201.

[48] X.X. Han, G.G. Huang, B. Zhao, Y. Ozaki, Anal. Chem. 81 (2009) 3329–33.

[49] J. Moger, P. Gribbon, a Sewing, C.P. Winlove, Biochim. Biophys. Acta 1770 (2007) 912–8.

[50] J. Gao, H. Gu, F. Liu, X. Dong, M. Xie, Y. Hu, J. Mol. Struct. 998 (2011) 171–178.

[51] Y. Rao, Q. Chen, J. Dong, W. Qian, Analyst 136 (2011) 769–774.

[52] M. Dendisova-Vyskovska, G. Broncova, M. Clupek, V. Prokopec, P. Matejka, Spectrochim. Acta - Part A Mol. Biomol. Spectrosc. 99 (2012) 196–204.

[53] J.A. Creighton, C.G. Blatchford, M.G. Albrecht, J. Chem. Soc., Faraday Trans. 2 75 (1979) 790–798.

[54] X. Chen, H. Gu, G. Shen, X. Dong, J. Kang, J. Mol. Struct. 975 (2010) 63–68.

[55] W. Meng, F. Hu, X. Jiang, L. Lu, Nanoscale Res. Lett. 10 (2015) 1–8.

[56] G. Das, F. Gentile, M.L. Coluccio, A.M. Perri, A. Nicastri, F. Mecarini, G. Cojoc, P. Candeloro, C. Liberale, F. De Angelis, E. Di Fabrizio, in:, J. Mol. Struct., 2011, pp. 500–505.

[57] S. V. Sokolov, K. Tschulik, C. Batchelor-McAuley, K. Jurkschat, R.G. Compton, Anal. Chem. 87 (2015) 10033–10039.

[58] A. Barbara, F. Dubois, A. Ibanez, L.M. Eng, P. Quémerais, J. Phys. Chem. C 118 (2014) 17922–17931.

[59] S. Agnihotri, S. Mukherji, S. Mukherji, RSC Adv. 4 (2014) 3974–3983.

[60] D.D. Evanoff, G. Chumanov, ChemPhysChem 6 (2005) 1221–1231.

[61] D. Paramelle, A. Sadovoy, S. Gorelik, P. Free, J. Hobley, D.G. Fernig, Analyst 139 (2014) 4855–61.

[62] K.B. Mogensen, K. Kneipp, J. Phys. Chem. C 118 (2014) 28075–28083.

[63] Y. Xiaojuan, G. Huaimin, W. Jiwei, J. Mol. Struct. 977 (2010) 56–61.

[64] J.S. Suh, M. Moskovits, J. Am. Chem. Soc. 108 (1986) 44711–4718.

[65] A. Sabur, M. Havel, Y. Gogotsi, J. Raman Spectrosc. 39 (2008) 61–67.

[66] Shiohara Amane, Y. Wang, L.M. Liz-Marzán, J. Photochem. Photobiol. C Photochem. Rev. 21 (2014) 2–25.

[67] C.P. Shaw, M. Fan, C. Lane, G. Barry, A.I. Jirasek, A.G. Brolo, J. Phys. Chem. C 117 (2013) 16596–16605.

[68] V.R.R. Cunha, V.R.L. Constantino, R.A. Ando, Vib. Spectrosc. 58 (2012) 139–145.

[69] J.L. Castro, M.R. López Ramírez, I. López Tocón, J.C. Otero, J. Colloid Interface Sci. 263 (2003) 357–363.

[70] X. Dou, Y.M. Jung, Z.Q. Cao, Y. Ozaki, Appl. Spectrosc. 53 (1999) 1440–1447.

[71] E.C. Le Ru, E.J. Blackie, M. Meyer, P.G. Etchegoin, J. Phys. Chem. C 111 (2007) 13794–13803.

[72] U.K. Sarkar, Chem. Phys. Lett. 374 (2003) 341–347.

[73] S.P. Ozkorucuklu, J. Beltrán, G. Fonrodona, D. Barrón, G. Alsancak, J. Barbosa, J. Chem. Eng.

Data 54 (2009) 807–811.

[74] I. Pavel, a Szeghalmi, D. Moigno, S. Cîntă, W. Kiefer, Biopolymers 72 (2003) 25–37.

[75] C.-B. Wang, G. Deo, I.E. Wachs, J. Phys. Chem. B 103 (1999) 5645–5656.

[76] G.I.N. Waterhouse, G.A. Bowmaker, J.B. Metson, Appl. Surf. Sci. 214 (2003) 36–51.

[77] L. Wu, Z. Wang, S. Zong, Z. Huang, P. Zhang, Y. Cui, Biosens. Bioelectron. 38 (2012) 94–99.

CAPTIONS

Scheme 1. Structure and pKa values of the phenolic antioxidants studied.

Fig. 1. A) UV-Vis spectra of the synthesized Ag colloids. B) Representative TEM micrographs of colloids with high and low levels of aggregation (Left and right). C) PCA score plot and D) PCA loadings.

Fig. 2. Comparison of normal Raman and SERS spectra of Gly adsorbed on several Ag colloids. These colloids are circled in the PCA scatter plot. Gly concentration was 1 M for normal Raman and $2.5x10^{-3}$ M for SERS test. Both measurements were carried out in solution. Spectra are ordered from highest to lowest signal enhancement.

Fig. 3. SERS (7.5×10^{-6} M), Ag colloid blank and normal Raman spectra (1M) of CA, FA, pCA and SA. The Ag colloid blank consists of 2.56% of EtOH, 97.44% of AgNP colloid and was adjusted to pH 6.44 with HNO_3. Spectra are average of 5 individual measurements.

Fig. 4. Dependence of SERS intensity on the pH value. Concentration was fixed at $7.5x10^{-6}$M and the pH was modified from 2 to 12 and the SERS spectra were acquired for each value. The area under the curve was calculated for peaks in the region between 1100 and 1700 cm^{-1}.

Fig. 5. Concentration dependent SERS spectra of FA, pCA, SA and CA adsorbed onto Ag colloids.

Fig. 6. Calibration curves for of CA, pCA, FA and SA from (A) $2.5x10^{-9}$ M to $2.5x10^{-7}$ M and (B) $2.5x10^{-9}$ M to $7.5\ x10^{-6}$ M.

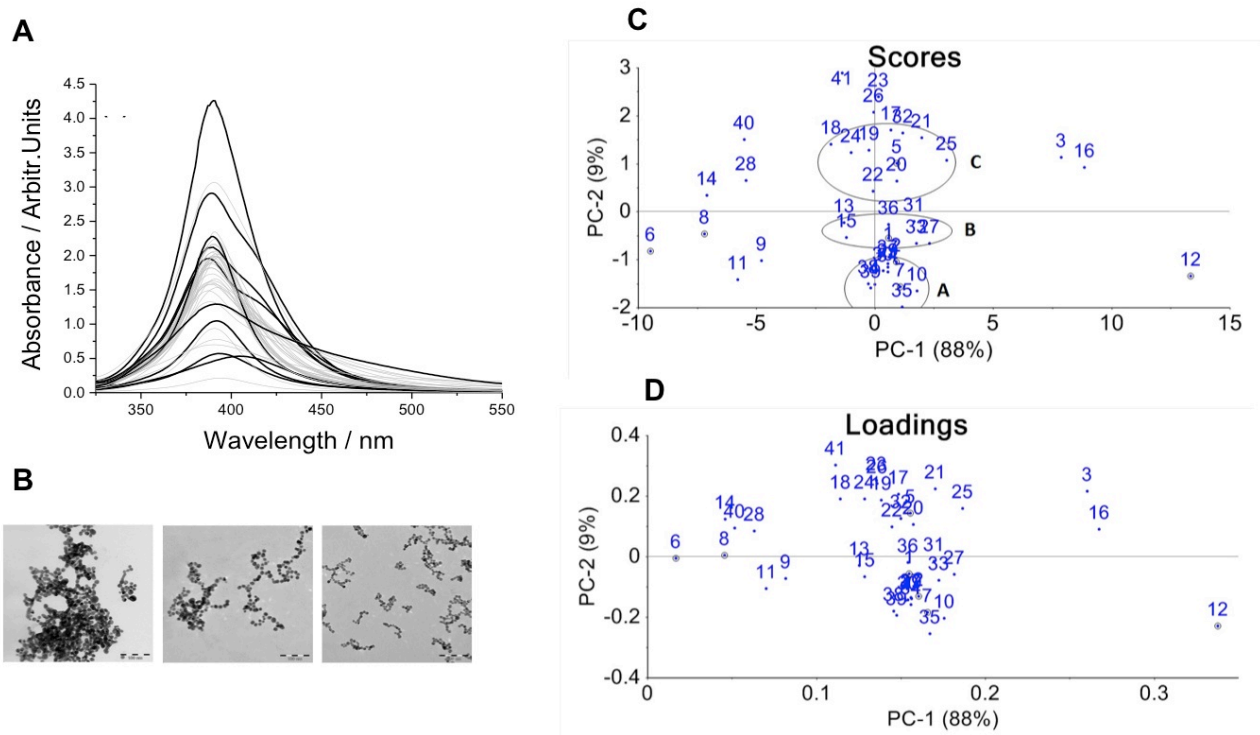
A
Absorbance / Arbitr.Units
Wavelength / nm
B
C
Scores
PC-2 (9%)
PC-1 (88%)
A
B
C
D
Loadings
PC-2 (9%)
PC-1 (88%)

Fig. 1

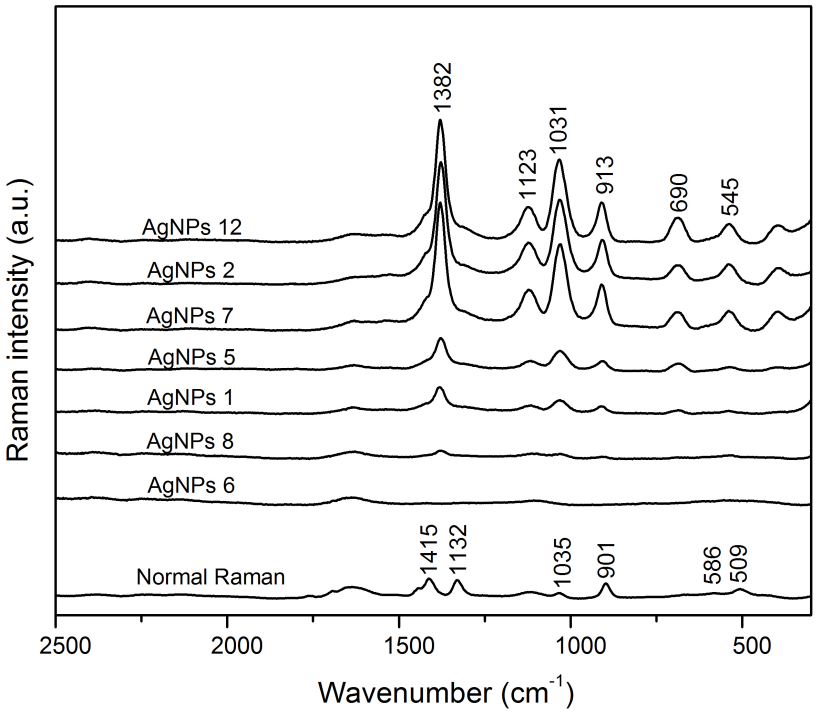
Raman intensity (a.u.)
AgNPs 12
AgNPs 2
AgNPs 7
AgNPs 5
AgNPs 1
AgNPs 8
AgNPs 6
Normal Raman
1382
1123
1031
913
690
545
1415
1132
1035
901
586
509
2500
2000
1500
1000
500
Wavenumber (cm-1)

Fig. 2

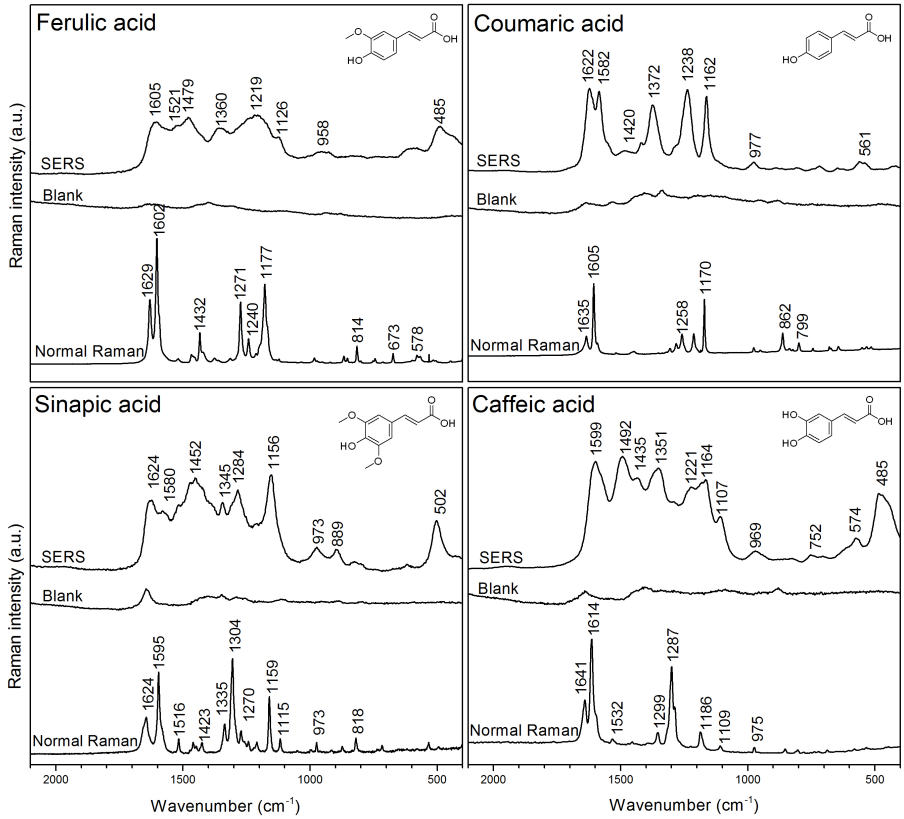
Ferulic acid
SERS
Blank
Normal Raman
1605
1521
1479
1360
1219
1126
958
485
1629
1602
1432
1271
1240
1177
814
673
578
Coumaric acid
1622
1582
1420
1372
1238
1162
977
561
1635
1605
1258
1170
862
799
Sinapic acid
1624
1580
1452
1345
1284
1156
973
889
502
1595
1516
1423
1335
1304
1270
1159
1115
973
818
Caffeic acid
1599
1492
1435
1351
1221
1164
1107
969
752
574
485
1641
1614
1532
1299
1287
1186
1109
975
Raman intensity (a.u.)
Wavenumber (cm-1)
2000
1500
1000
500

Fig. 3

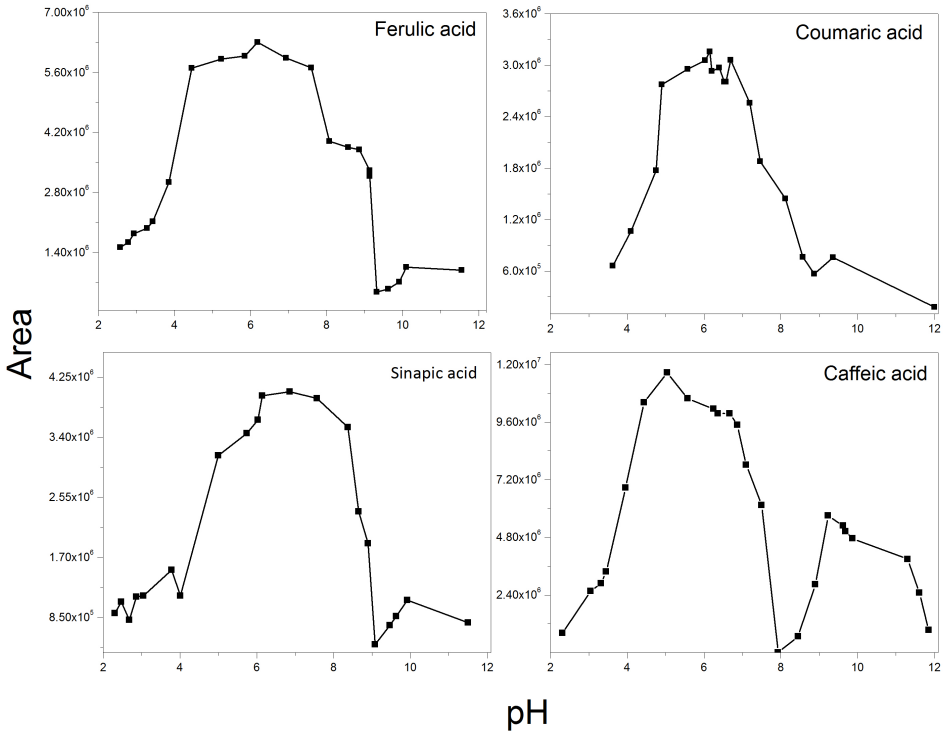
Ferulic acid
Coumaric acid
Sinapic acid
Caffeic acid
Area
pH

Fig.4

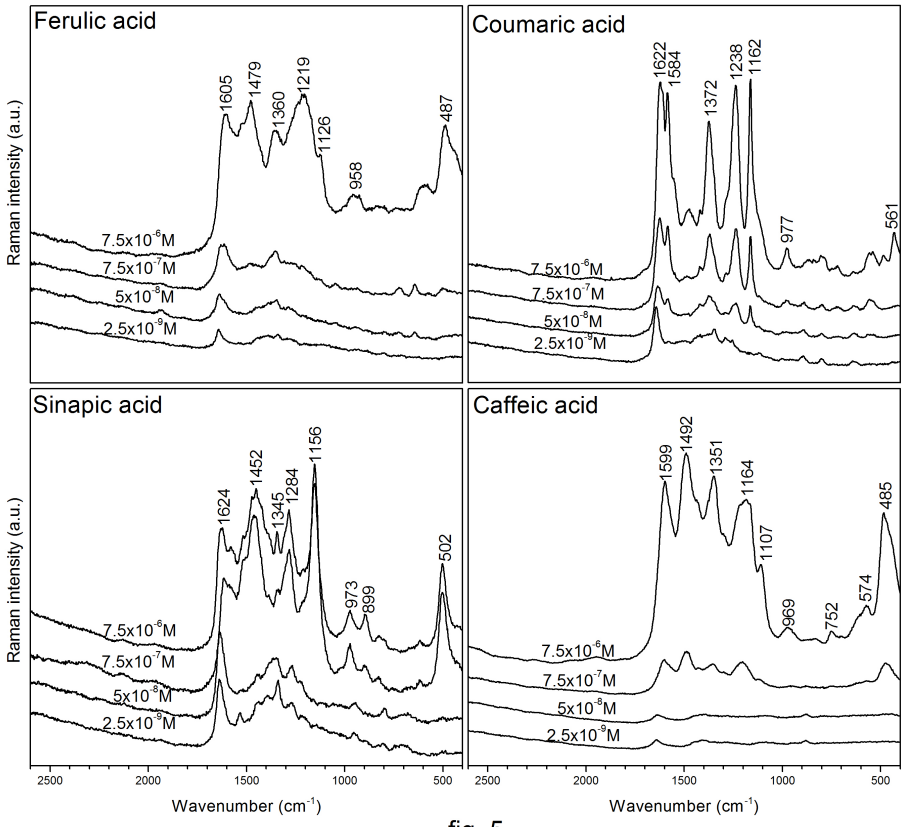
Ferulic acid
1605
1479
1360
1219
1126
958
487
7.5x10-6M
7.5x10-7M
5x10-8M
2.5x10-9M
Coumaric acid
1622
1584
1372
1238
1162
977
561
7.5x10-6M
7.5x10-7M
5x10-8M
2.5x10-9M
Sinapic acid
1624
1452
1345
1284
1156
973
899
502
7.5x10-6M
7.5x10-7M
5x10-8M
2.5x10-9M
Caffeic acid
1599
1492
1351
1164
1107
969
752
574
485
7.5x10-6M
7.5x10-7M
5x10-8M
2.5x10-9M
Raman intensity (a.u.)
Raman intensity (a.u.)
2500
2000
1500
1000
500
Wavenumber (cm-1)
Wavenumber (cm-1)

fig. 5

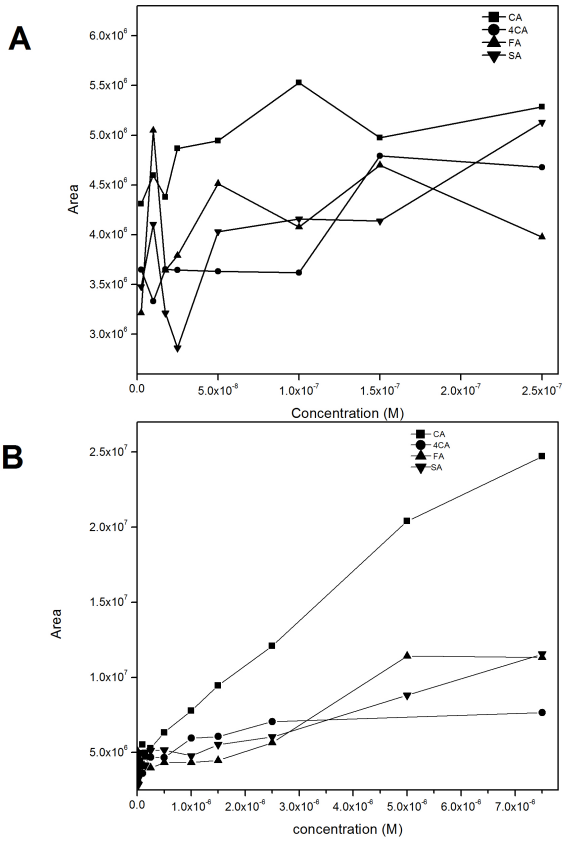
A
CA
4CA
FA
SA
Area
Concentration (M)
B
CA
4CA
FA
SA
Area
concentration (M)

Fig. 6